



Study of plasma parameters of coaxial plasma source using triple Langmuir probe and Faraday cup diagnostics

Sunil KANCHI^{1,2}, Rohit SHUKLA^{1,2}  and Archana SHARMA^{1,2,3} 

¹ Pulsed Power and Electromagnetics Division, Bhabha Atomic Research Centre, Visakhapatnam 531011, India

² Homi Bhabha National Institute, Mumbai 400085, India

³ Beam Technology Development Group, Bhabha Atomic Research Centre, Mumbai 400085, India

E-mail: sunilkanchi8125@gmail.com

Received 2 August 2023, revised 22 November 2023

Accepted for publication 22 November 2023

Published 11 April 2024



Abstract

Coaxial plasma guns are a type of plasma source that produces plasma which propagates radially and axially controlled by the shape of the ground electrode, which has attracted much interest in several applications. In this work, a 120° opening angle of CPG nozzle is used as a plasma gun configuration that operates at the energy of 150 J. The ionization of polyethylene insulator between the electrodes of the gun produces a cloud of hydrogen and carbon plasma. The triple Langmuir probe and Faraday cup are used to measure plasma density and plasma temperature. These methods are used to measure the on-axis and off-axis plasma divergence of the coaxial plasma gun. The peak values of ion densities measured at a distance of 25 mm on-axis from the plasma gun are $(1.6 \pm 0.5) \times 10^{19} \text{ m}^{-3}$ and $(2.8 \pm 0.6) \times 10^{19} \text{ m}^{-3}$ for hydrogen and carbon plasma respectively and the peak temperature is $3.02 \pm 0.5 \text{ eV}$. The mean propagation velocity of plasma is calculated using the transit times of plasma at different distances from the plasma gun and is found to be $4.54 \pm 0.25 \text{ cm}/\mu\text{s}$ and $1.81 \pm 0.18 \text{ cm}/\mu\text{s}$ for hydrogen and carbon plasma respectively. The Debye radius is obtained from the measured experimental data that satisfies the thin sheath approximation. The shot-to-shot stability of plasma parameters facilitates the use of plasma guns in laboratory experiments. These types of plasma sources can be used in many applications like plasma opening switches, plasma devices, and as plasma sources.

Keywords: coaxial plasma source, triple Langmuir probe, Faraday cup, plasma density, plasma temperature

(Some figures may appear in colour only in the online journal)

1. Introduction

Coaxial plasma guns (CPG) are the ion sources in the plasma opening switches that generate the plasma using the insulator's surface breakdown. These CPGs come under the erosional type of plasma generators in which material enters the regime of ionization and acceleration, resulting in the evaporation of insulators [1, 2] or electrode material [3, 4]. These CPGs have the advantage of obtaining high-energy plasmas eliminating the pulsed gas vents that require the accurate operation of electromagnetic valves involved in gas supply

lines [5] and laser-produced plasma systems [6] without compromising the requirements of plasma source parameters. The requirements include (i) minimization of background plasma perturbations, (ii) reduction in the interference due to high voltage breakdown on insulators, (iii) plasma cloud formation in the background plasma for the reproduction of space conditions [2], (iv) reproducibility, i.e., production of same plasma parameters for the shot to shot and (v) long life span to be used for laboratory experiments and in many applications. The insulators used in CPGs include polyethylene [2], plexiglas [7], etc. The CPGs

that meet the above requirements and are simple in construction are usually made of coaxial cables with an insulator as low-density polyethylene (LDPE) and provide high-voltage insulation between the electrodes. In this work, the CPG is made using RG-218 coaxial cable with polyethylene (PE) insulation.

2. Experimental setup

Figure 1(a) shows the electrical schematic of experimental setup of the capacitor discharge circuit for firing the plasma gun, and figure 1(b) shows the schematic of the plasma gun used in experiments. The electrical circuit consists of a capacitor 1 μ F, 25 kV, a triggered spark gap (SG) switch [8, 9], and a resistance of 20 k Ω parallel to the CPG. The coaxial cable has an inner copper conductor with a diameter of 4.95 mm, a PE insulator thickness of 6.16 mm, and the gun nozzle used is 120° opening angle. The acceleration gap between the inner conductor and outer CPG nozzle is 7.5 mm. The plasma is ejected and accelerated with the self-generated Lorentz force, i.e., $\mathbf{J} \times \mathbf{B}$ force from the electrodes, where \mathbf{J} is the current density, and \mathbf{B} is the magnetic field produced due to the current. The experiments are carried out in vacuum chamber evacuated to 4×10^{-4} mbar. The plasma chamber used in the experiments has diameter of 250 mm and height 220 mm. The parameters that are more important for the characterization of CPGs are plasma density (n_i), temperature (T_e), and plasma velocity. These parameters are measured using the triple Langmuir probe and Faraday cup methods discussed in sections 3 and 4, respectively.

3. Theory of triple Langmuir probe

For the characterization of a plasma gun, a triple Langmuir probe (TLP) was used against the plasma source for measuring plasma density (n_i) and temperature (T_e). This measurement method directly exhibits the plasma parameters using the microsecond intrinsic response time of the probe and avoids the difficulties of obtaining the I - V curve by the fast sweeping of bias voltage. The probe electrodes have differ-

ent profiles, including cylindrical, spherical, and planar [10]. Using various combinations of electrode profiles for probe design gives the asymmetric arrangement [11, 12], and using of same electrode profiles gives the symmetric arrangement [13]. In the present experimental study, the probe is designed with cylindrical electrodes with a symmetric arrangement. A cylindrical probe is a piece of wire that should have a high melting point and mechanical strength. The materials reported in the literature for probe design are tantalum, molybdenum, graphite, and tungsten [14]. In the symmetric arrangement, the two adjacent probes are negatively DC-biased, and the third probe is in floating mode. The voltage signal across the biased probes is proportional to the density (n_i), and the voltage signal between the high potential probe and the floating probe is proportional to the temperature (T_e). The ion saturation current (I_s) is obtained for the strong negatively biased potential that gives ion density (n_i), and the potential in which the current drawn is zero, known as floating potential and indicates the electron temperature (T_e). Depending on the electrical circuit connections, the TLP can be operated in (i) current and (ii) voltage mode [15]. The voltage mode TLP requires two DC power supplies, and the current mode TLP requires a single DC power supply, reducing the complexity of biasing the circuit and directly displaying the T_e and n_i . The theoretical considerations of the Langmuir probe are: (i) the plasma is in Maxwellian distribution, (ii) the probe dimension (r) is much larger than Debye length (λ_d), and (iii) the surface area of the probe must be small to minimize the perturbations due to plasma [16–18].

Figure 2(a) shows the electrical circuit of the current mode operation of TLP, which is used in the present experimental work. The plasma from the CPG hits the TLP in which two probe tips are biased at some potential. The potential attracts the unlike charges and repels the like-charged particles. These particles form a thin sheath on the surface of the probe tips. As per the theoretical considerations of the Langmuir probe, $r \gg \lambda_d$ defines the surface area of the probe exposed to plasma as the measuring area of the probe. When the charge particles are collected on the probe, the current flows through the circuit, and the ion current density is assumed to remain constant at all probe potentials; using the following equation, one may determine the plasma temperature [19, 20] as

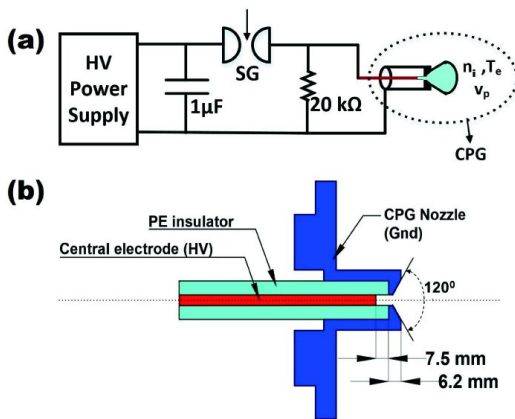


Figure 1. (a) Schematic of firing circuit. (b) CPG (not to the scale).

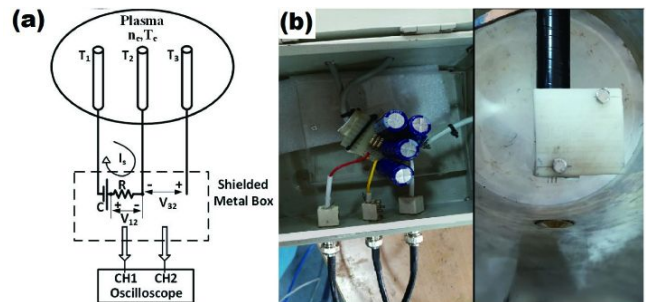


Figure 2. (a) Electrical schematic of TLP, and (b) experimental setup of the biasing circuit (left) and probe installed in a vacuum chamber (right).

$$kT_e = \frac{eV_{32}}{\ln(2)}, \quad (1)$$

where kT_e is the electron temperature in eV, e is the charge of an electron, and V_{32} is the voltage measured between positively biased probe T_2 and floating probe T_3 . The temperature measurement is independent of the type of ions in the plasma. The bias voltage across the probes T_1 and T_2 must be sufficiently high so that more ions are collected at the probe to get the ion saturation current such that $kT_e \ll eV_{12}$ [21] is satisfied. Using the values of $I_s = \frac{V_{12}}{R}$ (R is the resistance connected between probes T_1 and T_2) and kT_e , the plasma density can be estimated using the equation [16, 19]

$$n_i = \exp(0.5) \left(\frac{m_i}{kT_e} \right)^{0.5} \frac{I_s}{eA_p}, \quad (2)$$

where m_i is the mass of the ion and $A_p = 2\pi rl$ is the surface area of the tungsten probe exposed to plasma, r and l are the radius and length of the tungsten probe.

3.1. TLP design and installation

The TLP was designed in-house using three pieces of 480 μm diameter tungsten wire and a length of 10 mm exposure to plasma. These are connected to Teflon wires on other sides for signal collection and biasing the TLP. The tungsten wires are made rigid inside the Teflon rod of 20 mm diameter and length of 35 mm with 2.8 mm spacing between them. The whole assembly of TLP is passed through a plastic pipe and shielded with metal foil till the Teflon wires are connected to the three BNC feed-throughs inside the vacuum chamber. The RG58 coaxial cables connect the biasing circuit and the TLP. The biasing circuit used in the experiments is a capacitor-based circuit. The electrical schematic circuit of TLP is shown in figure 2(a), and the experimental setup is shown in figure 2(b). The capacitance C is 1 mF, 140 V rated charged using the stabilized power supply, and the circuit's series resistance, R , is 0.38 Ω . Electromagnetic noises during the discharge are more likely to affect these circuits, so the biasing circuit is covered with aluminium foil and is installed in a metal box. When the TLP is unbiased, there will be no current flowing in the biased path, and when the TLP is biased, probe T_2 will have a potential less than T_3 , and due to the flow of ions, the current I_s passes through the resistor R . The potential drop across R is measured using the oscilloscope with which the I_s can be calculated. During the measurements, the oscilloscope is isolated from the metal box such that high voltage ground is isolated from the oscilloscope.

4. Theory of Faraday cup

Faraday cups (FCs) are charge collector devices that collect the charged particles in a vacuum and are used to give the

time histories of the particles when kept against the plasma source. Optimized design of FC is a challenging task for specific applications, even if it is simple in construction and a reliable technique for measuring beam current and the plasma density of the source [22, 23]. Different types of FC designs are reported in the literature depending on the application [24, 25]. Care must be taken in designing the FC because the back-scattered and secondary emission electrons (SEE) are emitted from the surface of the collector when the charged particles impact electrodes, and these secondary electrons may escape from the FC aperture for high-energy plasma sources. The escape of electrons results in the underestimation of beam current for negative ions or electrons and the overestimation of beam current for positively charged particles [22]. The reduction in the loss probability of secondary capture electrons is made by optimizing the dimensions of FC and using low Z material can be considered while designing the FC [26, 27]. The schematic of the electrical circuit of FC is shown in figure 3. The ion density using FC can be estimated by equation

$$n_{iFC} = \frac{I_{FC}}{A_{FC}v_iZe}, \quad (3)$$

where $I_{FC} = \frac{V_{FC}}{R_t}$ is the current flowing through terminating resistance R_t , V_{FC} is the voltage measured by oscilloscope across R_t , A_{FC} is the input hole area, v_i is the velocity of ions obtained using plasma transit times, Z is the charge state of respective ion and e is charge of the electron.

4.1. Faraday cup design

The Faraday cup consists of two electrodes arranged concentrically and isolated electrically by a Kepton insulator, shown in figure 3. The inner electrode (collector) is 4.8 mm in diameter, the insulator is 0.1 mm thick, and the metal casing is 20 mm in diameter and 25 mm in length. The electrodes are made of brass. The collector is negatively biased using a capacitor-based circuit through 5 M Ω resistance and the capacitor (C) is charged using stabilized power supply. Geometrically low aperture-to-length ratio, i.e., the deep cup-shaped electrode arrangement, minimizes the loss of secondary electrons emitted from the collector when ions impact the inner electrode.

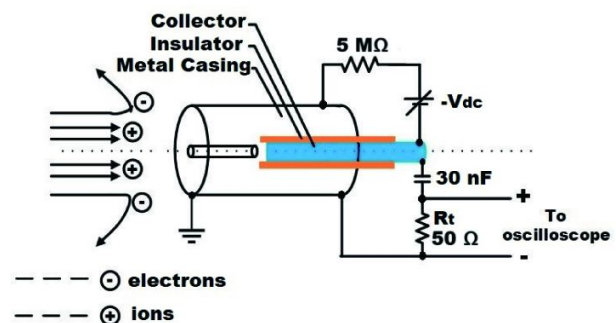


Figure 3. Electrical circuit of biasing circuit of FC.

4.2. Simulations of the Faraday cup

To assess the performance of the FC, numerical simulations have been performed using CST Particle Studio. The 3D CST model of the FC is shown in figure 4. The loss probability using the SE emission model is simulated. When FC is negatively biased, the potential is maximum at the surface of the metal casing and has the minimum value at the center along the axis of the beam. To know the loss probability of SE electrons, particle tracking simulations were run at different energies and by sweeping the voltage from 0 to 250 V. The collector surface is selected as the circular source. The emitted electrons are taken as $N_{emit} = 10200$ for every simulation run and emission energy E_e . From the aperture, some of the electrons are diverted to the collector due to the presence of an electric field called captured electrons N_{cap} , and the remaining electrons have high energy to overcome the potential barrier, which escapes from the aperture, and these electrons are denoted by $N_{escp} = N_{emit} - N_{cap}$. The loss probability of SEE is given by the equation (4)

$$\gamma = \frac{N_{escp}}{N_{emit}}. \quad (4)$$

The trajectories of electrons are shown in figure 5(a), and the loss probability of electrons as a function of E_e and bias voltage (V_{bias}) as $\gamma(E_e, V_{bias})$ is shown in figure 5(b). These simulations show the points from where the electron escape is maximum, and the electron trajectories can be determined. The parameter by which the performance of FC can be decided is the minimum energy E_{min} that the electron can escape from the aperture. Considering the columbic interaction, the SEE electrons have maximum energy given by equation [28]

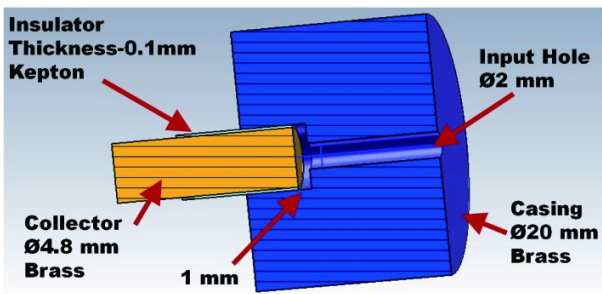


Figure 4. 3D CST model of FC.

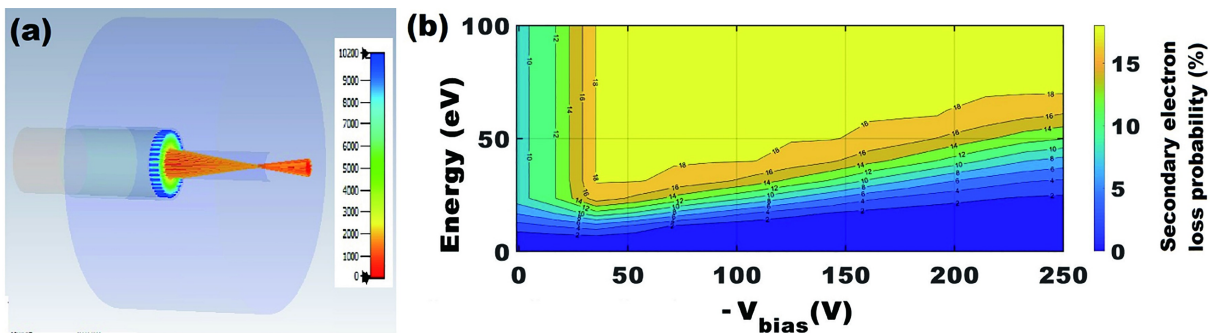


Figure 5. (a) SEE trajectories at 10 eV, (b) loss probability of SEEs.

$$E_{max} = 4 \frac{m_e m_i}{(m_e + m_i)^2} E_{ion} \cos^2 \phi, \quad (5)$$

where m_e and m_i are the mass of the electron and the ion, respectively, E_{ion} is the energy of the ion, and ϕ is the angle between incident ions and trajectory of ejected electrons. From equation (5), if the ions incident on the collector and the emitted electrons that are moving with an angle, $\phi = 180^\circ$, i.e., opposite to ions, then these electrons may have the maximum energy, and their velocity is entirely in the axial direction. Only these electrons have maximum chances to escape from an aperture that has energy E_{min} .

5. Results and discussion

Figure 1(a) shows the CPG firing circuit, and the voltage applied across the insulator produces the plasma, which initiates the temperature and density of the plasma. The vacuum chamber is evacuated to a pressure of 4×10^{-4} mbar. The capacitor $1 \mu F$ is charged to 17 kV and discharged through a spark-gap switch that ejects plasma through CPG. The ionization of the insulator surface, creation of ions and electrons, henceforth temperature and density depend on the discharge voltage pulse. The discharge current is monitored using the current monitor shown in figure 6(a), which has a peak current of 8 kA with a quarter cycle time period of $2 \mu s$.

5.1. Ion density and temperature measurements

The ion saturation signals are measured using the biasing circuits of TLP and FC shown in figures 2(a) and 3, respectively. The bias voltages for TLP and FC are -40 V and -150 V, respectively, and these voltages are found experimentally such that the saturation in the output is observed. These diagnostics were biased using a 1 mF polarized capacitor during the discharge process and biasing voltage is constant during total measurements. Figure 6(b) shows that the density waveforms measured at a distance of 50 mm from the plasma gun axially, have two peaks that appeared with some delay which indicates the ionization of polyethylene $[(C_2H_4)_n]$ insulator has the hydrogen (H^+) and carbon (C^+ , C^{++}) ions in the plasma as per the spectroscopic and charge

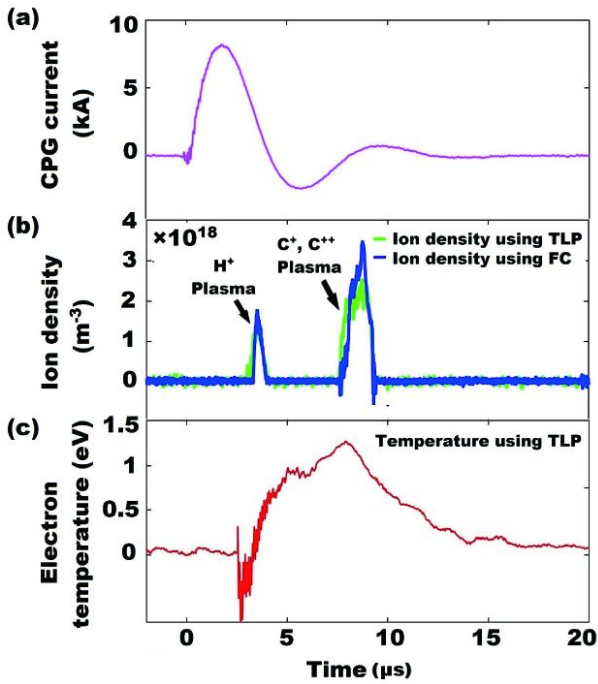


Figure 6. Experimental waveforms. (a) CPG discharge current, (b) ion density signals using TLP and FC, and (c) temperature measured using TLP at a distance of 50 mm.

collector studies in references [29, 30]. The parameters considered for calculation of density of hydrogen and carbon plasma respectively using TLP and FC are given in table 1. The peak density values of hydrogen and carbon ions at a distance of 25 mm from the plasma gun axially are $(1.6 \pm 0.5) \times 10^{19} \text{ m}^{-3}$ and $(2.8 \pm 0.6) \times 10^{19} \text{ m}^{-3}$, respectively, and as the plasma propagates, the density dropped with an increase in the distance from the CPG. At 50 mm, the den-

Table 1. Parameters of TLP and FC for calculation of density.

Parameter	Value
Mass of hydrogen ion	$1.67 \times 10^{-27} \text{ kg}$
Mass of carbon ion	$20 \times 10^{-27} \text{ kg}$
Charge state of hydrogen ion (Z)	1
Charge state of carbon ion (Z)	2
e	$1.602 \times 10^{-19} \text{ C}$
A_p	15.07 mm^2
A_{FC}	3.14 mm^2

ties of the hydrogen and carbon ions decreased to $(3.57 \pm 3.22) \times 10^{18} \text{ m}^{-3}$ and $(5.65 \pm 5.20) \times 10^{18} \text{ m}^{-3}$, respectively. The plasma exhaust mean velocity is calculated from the plasma transit times at different distances. The mean velocities of hydrogen and carbon ions measured using transit times of plasma from 25 mm to 50 mm are $(4.54 \pm 0.25) \text{ cm}/\mu\text{s}$ and $(1.81 \pm 0.18) \text{ cm}/\mu\text{s}$, respectively.

The temperature trace is directly proportional to the voltage signal of the floating probe of the TLP biasing circuit. The T_e amplitude is based on the number of energetic electrons hitting the floating probe and will vanish after the plasma is completed. The temperature signal is independent of the ions that hit the floating probe tip. The electromagnetic noises are less prominent on TLP measurements at lower magnitudes of discharge voltages [20]. Figure 6(c) shows the electron temperature waveform measured using TLP, which rises rapidly during the beginning of the pulse because the most energetic electrons emerge from the CPG region [18].

5.2. Radial and axial variations of n_i and T_e

For the characterization and to study the divergence of CPG, the FC and TLP are placed at different locations, as shown in figure 7. The diagnostics were placed on-axis axially and off-axis radially to study the CPG plasma parameters. The radial and axial directions are denoted as per plasma motion in the chamber. Figures 8(a) and (b) shows the n_i and T_e peak values as a function of the on-axis distances. As the diagnostic location is moved far away from the gun axially, the temperature and density decrease as expected due to rapid expansion of plasma and the recombination of ion-electron

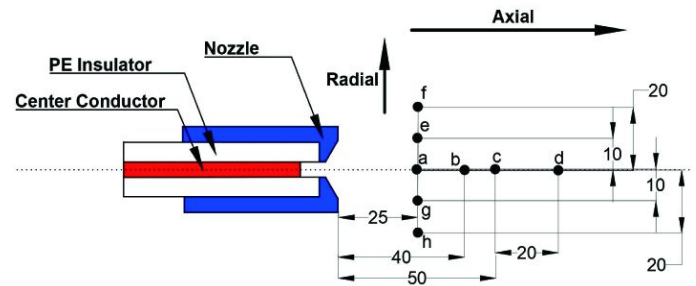


Figure 7. a, b, c, d are the on-axis locations and e, f, g, h are the off-axis locations of plasma diagnostics.

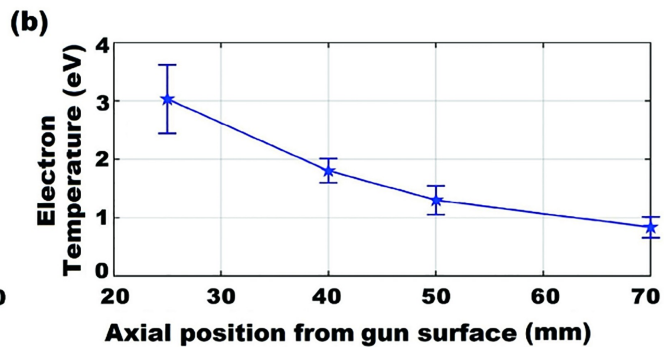
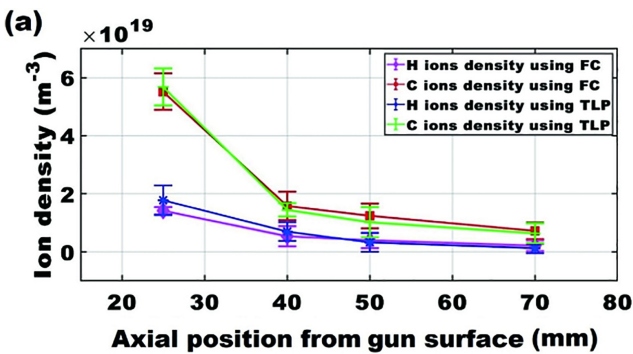


Figure 8. Axial (on-axis) variations of (a) n_i and (b) T_e .

pairs [31]. The peak density values of hydrogen and carbon ions that occurred at different distances are represented in figure 8(a), and the carbon ion density is higher than the hydrogen ions density. These results indicate the propagation of plasma at longer distances. The off-axis measurements of plasma parameters are determined by placing the plasma diagnostics at locations e, f, g, and h, as shown in figure 7. The locations e and g are +10 mm and -10 mm, respectively, and f and h are +20 mm and -20 mm, respectively, at a distance of 25 mm from the gun axially denoted by 0 on the x -axis in figure 9(a). The n_i and T_e decrease on both sides of off-axis measurements as shown in figures 9(a) and (b). These measurements are more important in maintaining the dependable values of n_i and T_e as plasma propagates along the on-axis and may contribute to the optimum thrust of plasma. These studies play a significant role in deciding the plasma bridge length in the operation of plasma opening switch experiments.

The Debye radius (λ_d) of plasma is an essential parameter in plasma science and is the minimum radius required to satisfy the charge neutrality condition [32]. The values of n_i and T_e obtained from experimental data are used to determine the Debye radius of the plasma and obtained using the formula

$$\lambda_d = \left(\frac{\epsilon_0 k T_e}{n_i e^2} \right)^{1/2}, \quad (6)$$

where k is the Boltzmann constant, ϵ_0 is the permittivity of free space, T_e is the electron temperature, n_i is the charged particle number density, and e is the electron charge. Table 2 gives the data obtained at 17 kV charging voltage and at position 'a' in figure 7. The factor r/λ_d is calculated to be approximately ~ 526 , which shows that the Debye radius is much smaller than the probe radius. This indicates that the dimensions employed to fabricate TLP satisfy the thin sheath approximation. So, the surface area of the probe used to

expose the plasma can be considered as measurement region of the plasma parameters.

6. Conclusion

The plasma density and temperature are the essential plasma characteristics to be studied for CPGs. In this work, the plasma parameters are measured using the triple Langmuir probe and Faraday cup methods. The TLP gives the traces of plasma density and temperature; the Faraday cup only provides information about plasma density. The voltage applied across the two electrodes with polyethylene as the insulator ionizes and produces the hydrogen plasma and carbon plasma, and these plasmas do not interact with each other as they appear at different times. These two ions are observed as the peaks appearing in the density profiles verified by TLP and FC. The maximum density and temperature that occur at 25 mm on-axis measurements from CPG and decrease as the plasma propagates, and values are $(1.6 \pm 0.5) \times 10^{19} \text{ m}^{-3}$ and $(2.8 \pm 0.6) \times 10^{19} \text{ m}^{-3}$ for hydrogen and carbon ions, and the temperature is $(3.02 \pm 0.5) \text{ eV}$. The mean velocities measured using plasma transit times are $(4.54 \pm 0.25) \text{ cm}/\mu\text{s}$ and $(1.81 \pm 0.18) \text{ cm}/\mu\text{s}$ for hydrogen and carbon ions, respectively. The variation of plasma parameters radially and axially was studied, and hence these measurements afforded an overall view of how CPG plasma expands and the plasma parameters vary with time and distance, which could facilitate further experiments on CPGs. The experiments shows high reproducibility of plasma parameters from shot to shot. CPG method of plasma generation is a low-cost method and also has control over the density and velocity by varying the insulator length and charging voltage and the temperature by increasing the energy. These parameter studies play a critical role in knowing the plasma bridge length on the cathode electrode of plasma opening switches, and these switches

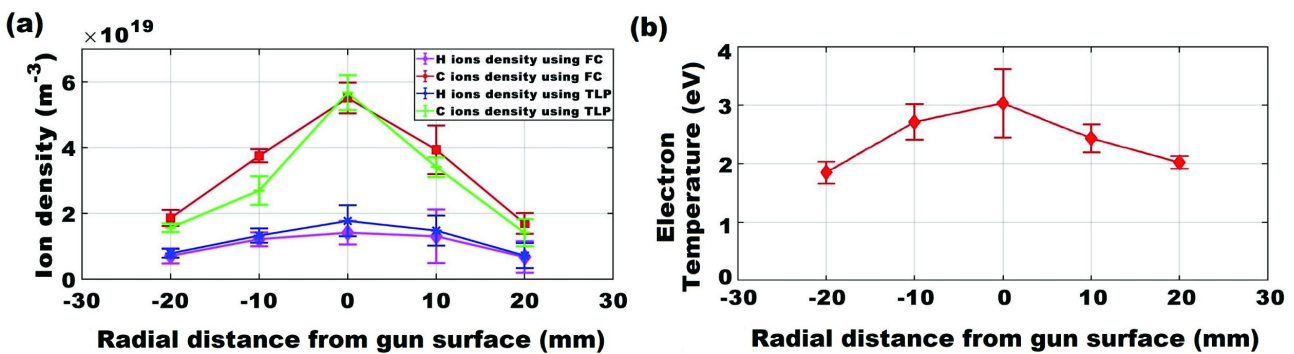


Figure 9. Radial (off-axis) variations of (a) n_i and (b) T_e from the gun.

Table 2. Estimation of Debye radius using n_i and T_e .

Voltage (kV)	Plasma density using TLP, n_i (m^{-3})		Plasma temperature, T_e (eV)	Debye radius, λ_d (μm)		Radius of TLP probe, r (mm)	r/λ_d
	Hydrogen plasma	Carbon plasma		Hydrogen plasma	Carbon plasma		
17	1.6×10^{19}	2.8×10^{19}	3.02	0.91	0.68	0.48	526.82

can operate for a higher range of currents depending on the optimized parameters of the plasma source.

Acknowledgments

This work was supported by Bhabha Atomic Research Centre, Department of Atomic Energy, Government of India. Authors would like to thank Premananda Dey, A. K. Dubey, K. Sagar and K. Venkata Apparao for their kind support. One of the author, Sunil Kanchi would like to thank Department of Atomic Energy, Government of India for financial assistance under DAE Doctoral Fellowship Scheme-2018.

ORCID iDs

Rohit SHUKLA  <https://orcid.org/0000-0002-1920-2556>
Archana SHARMA  <https://orcid.org/0000-0002-6705-0446>

References

- [1] Witherspoon F D *et al* 2009 *Rev. Sci. Instrum.* **80** 083506
- [2] Korobkov S V *et al* 2019 *Tech. Phys. Lett.* **45** 228
- [3] De La Fuente H and Forsen H 1971 *Rev. Sci. Instrum.* **42** 1453
- [4] Mendel C W Jr *et al* 1980 *Rev. Sci. Instrum.* **51** 1641
- [5] Ananjin P S *et al* 1992 *IEEE Trans. Plasma Sci.* **20** 537
- [6] Akiyama H *et al* Plasma erosion opening switch using laser-produced plasma In: *1992 9th International Conference on High-Power Particle Beams: IEEE 1992: vol 1 (IEEE)* p 627
- [7] Gavrilov B G, Kozhukhov S A and Sobyenin D B 1994 *Techn. Phys.* **39** 543
- [8] Kanchi S, Shukla R and Sharma A 2020 *Rev. Sci. Instrum.* **91** 104704
- [9] Kanchi S, Shukla R and Sharma A 2023 *IEEE Trans. Plasma Sci.* **51** 1959
- [10] Bhattarai S and Mishra L N 2017 *Int. J. Phys.* **5** 73
- [11] Mackel F *et al* 2011 *Meas. Sci. Technol.* **22** 055705
- [12] Mikoshiba S and Nakano Y 1968 *Jpn. J. Appl. Phys.* **7** 311
- [13] Eckman R *et al* 2001 *J. Propul. Power* **17** 762
- [14] Conde L 2011 An introduction to langmuir probe diagnostics of plasmas Tech. rep. Dept. Física. ETSI Aeronáut ingenieros Aeronáuticos Universidad Politécnica de Madrid, Spain
- [15] Polzin K A *et al* Behavior of triple langmuir probes in non-equilibrium plasmas In: *AIAA Propulsion and Energy 2019 Forum Indianapolis: AIAA 2019* p 3990
- [16] Qayyum A *et al* 2015 *J. Fusion Energy* **34** 405
- [17] Lee H C *et al* 2021 *Vacuum* **187** 110135
- [18] Borthakur S *et al* 2018 *Phys. Plasmas* **25** 013532
- [19] Riccardi C *et al* 2001 *Rev. Sci. Instrum.* **72** 461
- [20] Singha S *et al* 2021 *IEEE Trans. Plasma Sci.* **50** 1440
- [21] Kamitsuma M, Chen S L and Chang J S 1977 *J. Phys. D: Appl. Phys.* **10** 1065
- [22] Naieni A K *et al* 2009 *Vacuum* **83** 1095
- [23] Bai X Y *et al* 2017 *Plasma Sci. Technol.* **19** 035003
- [24] Seamans J F and Kimura W D 1993 *Rev. Sci. Instrum.* **64** 460
- [25] Damideh V *et al* 2017 *Phys. Plasmas* **24** 063302
- [26] Pearlman J S 1977 *Rev. Sci. Instrum.* **48** 1064
- [27] Ebrahimibasabi E, Feghhi S and Khorsandi M 2012 Design and simulation of a new faraday cup for es-200 electrostatic accelerator In: *Proceedings of RUPAC2012, Saint-Petersburg, Russia*
- [28] Roshani G H, Habibi M and Sohrabi M 2011 *Vacuum* **86** 250
- [29] Douieb F 1995 Experimental study of a plasma opening switch of different geometry *PhD thesis Universite de Paris XI, Orsay*
- [30] Kumar R *et al* Plasma source for a miniature and repetitive plasma opening switch In: *2008 IEEE International Power Modulators and High-Voltage Conference Las Vegas: IEEE 2008: p 189*
- [31] Nehra V, Kumar A and Dwivedi H 2008 *Int. J. Eng.* **2** 53
- [32] Diver D A 2001 *A Plasma Formulary for Physics, Technology and Astrophysics* (Berlin: WileyVCH)